# Magnetic Holes in the Solar Wind

by

Paisa Seeluangsawat

Submitted to the Department of physics
in partial fulfillment of the requirements for the degree of

Bachelor of Science

at the

MASSACHUSETTS INSTITUTE OF TECHNOLOGY

June 2002



Author ..... .....
Department of physics
May 17, 2002

Certified by . .....
Dr. Alan J. Lazarus
Senior Research Scientist, Senior Lecturer
Thesis Supervisor

Accepted by ..... ...
Prof. David E. Pritchard
Senior Thesis Coordinator, Department of Physics

# Magnetic Holes in the Solar Wind

by

Paisa Seeluangsawat

Submitted to the Department of physics
on May 17, 2002, in partial fulfillment of the
requirements for the degree of
Bachelor of Science

## Abstract

We attempt to locate magnetic holes from several years of data collected from WIND and ACE spacecraft and use them to study some statistical properties of the magnetic holes.

Thesis Supervisor: Dr. Alan J. Lazarus
Title: Senior Research Scientist, Senior Lecturer

# Acknowledgments

The author and the work presented here have received much help from people at the MIT Space Plasma Group, especially from his supervisors Alan J. Lazarus and Justin C. Kasper.

# Contents

# List of Figures

# List of Tables

# Chapter 1

# Introduction

The solar wind is a completely ionized neutral gas (plasma) traveling radially outward from the Sun at a speed of about 300-1000 km/s. The charged particles in the solar wind drag with them the Sun's magnetic field, reaching Earth and well beyond. As Fig. 1-1 illustrates, this stretched field can create a plane with the magnetic field on each side pointing in opposite directions. Maxwell equations tell us that there is a current flowing along this plane $\vec{J} = \frac{1}{\mu_0}\vec{\nabla} \times \vec{B}$, hence its name "current sheet".

Since 1962, several spacecraft have been measuring the magnetic field and the plasma density and velocity. As the current sheet passes through a spacecraft, the magnetic field detector on board measures the reversal of the magnetic field direction. The total field strength may dip momentarily.

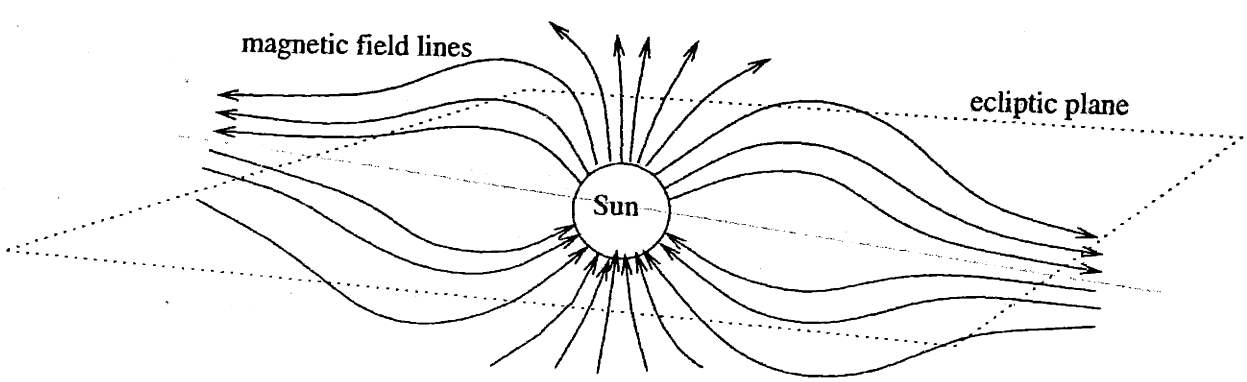


Figure 1-1: The Sun's magnetic field is extended by the solar wind.

However, only a small portion of such dips in magnetic field strength come with the field direction reversal. The dips without such a reversal are called "linear magnetic holes". Such holes are observed often. Most of them are small–at least as small as the monitoring detectors' sampling periods. The holes of sizes varying from 500 km to as large as $10^6$ km have been observed. The mechanism of their formation is still unclear.

Since many magnetic holes are found near a current sheet crossing, some believe that they originate from the current sheet. However, others believe that the holes originate within the sun or on its surface. Whether the magnetic holes originate from the sun, or later in interplanetary space is still not clear.

# Chapter 2

# Data

## 2.1 Acquisition

This study focuses on data collected from two spacecraft.

**Advanced Composition Explorer (ACE)** was launched on 25 August 1997 and stays at the first Lagrangian point (L1), which is about 1/100 on the way from Earth to the Sun (about 220 Earth radii ($R_e$) from Earth, $R_e = 6378.07\,\text{km}$). Here, the sum of the Earth's and the Sun's gravitation forces gives the right acceleration to orbit an object around the sun in one year, and hence it would appear stationary between the Earth and the Sun.

**(WIND)** was launched on on 1 November 1994. It runs an irregular path around Earth and L1. Parts of its orbit are inside the Earth's bowshock, which is the region where the solar wind is affected by the earth's magnetic field. We will ignore data in that region. WIND's distance upstream from a model of the bowshock is shown in Fig. 2-1.

Both spacecraft collect magnetic field strength and plasma velocity, among other data. Details on the instruments on board are available on their web pages ([1], [2], [3], [4]). Table 2.1 summarizes the data sampling rates.

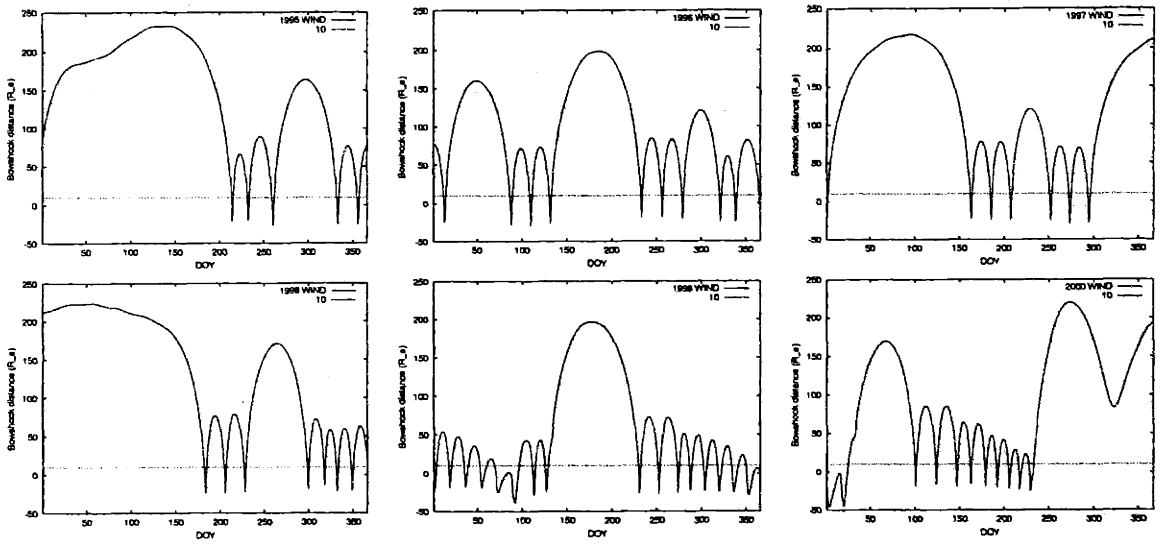

Figure 2-1: WIND's upstream distance from a bowshock model in years 1995-2000. We look for magnetic holes only when the spacecraft is more than $10R_e$ upstream from the model bowshock

| spacecraft | magnetic field (/sample) | | plasma velocity (/sample) | |
|---|---|---|---|---|
| | instrumental limit | available for analysis | instrumental limit | available for analysis |
| WIND | 22 ms | 3 s | 1.5 s | 85 - 105 s |
| ACE | 40 ms | 16 s | | 63 - 68 s |

Table 2.1: Sampling rate of data used in the analysis

## 2.2 Analysis Method

Data analysis is done in Interactive Data Language (IDL). Acquired data are available as a function call. I only need to specify dates and types of data wanted. The function returns all data points within the period.

# Chapter 3

# Hole Search

To study statistics of magnetic holes, first we need go through the magnetic field data we have (we will called this "signal") and locate the presence of holes.

## 3.1 What is a hole?

Common sense tells us that a hole occurs when the signal goes down and comes back up. Only that is too broad a definition. Random variations, both micro and macroscopic, as shown in Fig. 3-1 also fall into the description. We need a more specific definition.

To ignore small variations (will be called noise from here on), we can say the signal must drop pretty "deep", deeper than some threshold depth, before coming back up in order to be registered as a hole. But how should we set the threshold depth?

If we look for the signal to drop by some absolute threshold amount, say 1 nT, we will mistake big noises as holes, while missing a real hole with small drops. Fig.3-2 illustrates this. Setting a fractional threshold depth, like 40% drop, also leaves us with the same problems (Fig. 3-3). Hence, the threshold depth must be set relative to the noise level. The bigger the noise, the deeper the threshold depth.

The way we measure a drop is also important. An obvious method is taking the difference between the values at the current data point and the one before it. This method is fine when the hole is observed in a short time comparing to the sampling rate. For longer holes, this

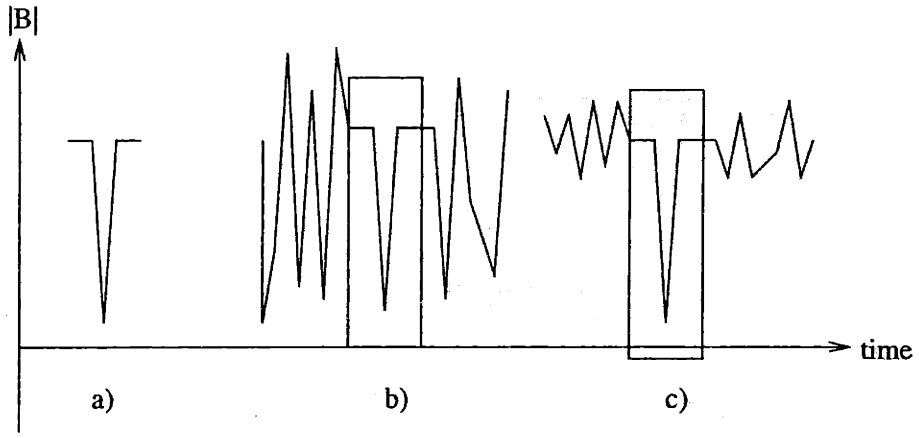


Figure 3-1: Down and up are too broad to be a definition for a hole.

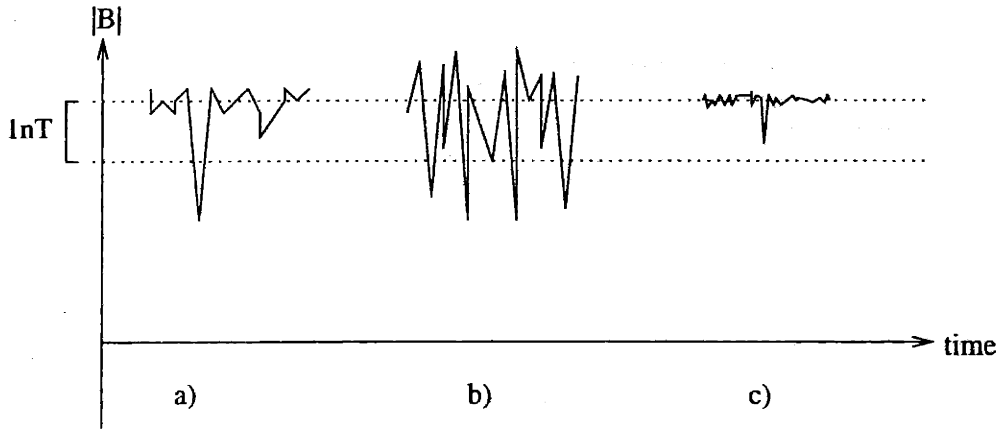


Figure 3-2: Setting an absolute threshold depth solves some noise problems (a), but mistakes big noises for holes (b), and misses tiny holes (c).

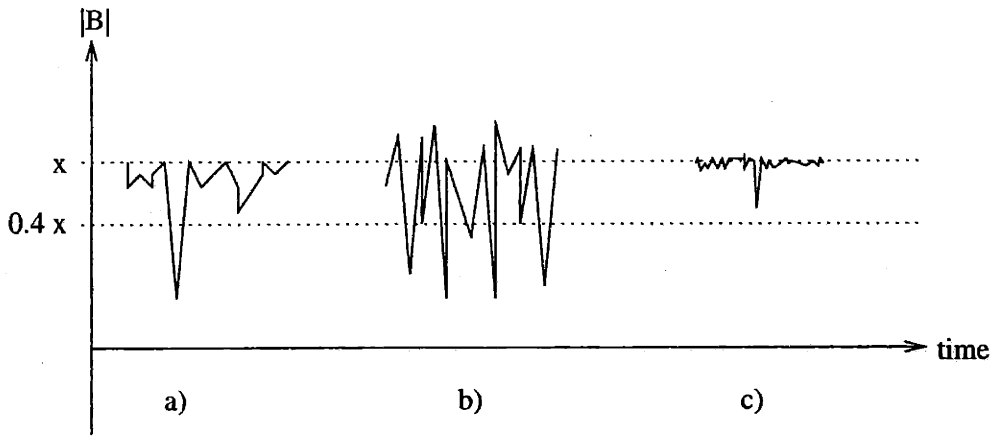


Figure 3-3: Setting a fractional threshold depth solves some signal noise problems (a), but mistakes big noises as holes (b), and misses tiny holes (c).

method will register only holes with steep edges (see Fig. 3-4).

We don't want to make the assumption that the drop is steep. After all, a gradual edge will look steep at a lower sampling rate. If we take the difference between current data point and the shoulder of the hole as the drop, the measured depth of a hole no longer depend on the steepness of the edge. But what should we take as the level of the hole's shoulder? After all, we still don't know where the holes are.

## 3.2 Method Used

In our method, we assume that each hole has relatively long and smooth shoulders comparing to the dip at the hole. That way, we can take the average of the data over some time ($\bar{x}$) as the shoulder level. Since most noise will stay within a few standard deviations ($\sigma$), we can take any drop below several $\sigma$'s as deep, and potentially a hole. Fig.3-5 illustrates this.

There are two big parameters to be set,

1. What should the averaging duration be?

2. How many standard deviations should we set as the threshold depth?

To answer this, let's look at a model of a hole (Fig. 3-6). Our hole model is a long and smooth signal, with a dip of magnetic strength $b$ for a duration $a$. If we take the averaging

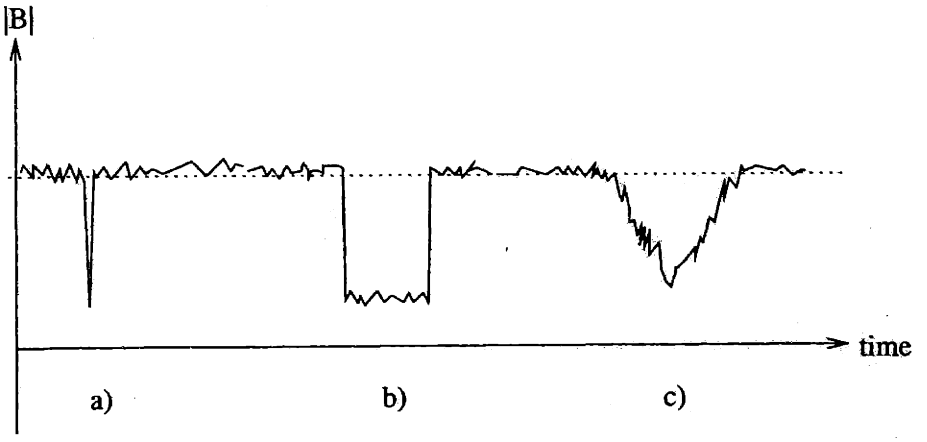


Figure 3-4: Taking the difference between consecutive data points as the drop work for some holes (a,b) but misses holes with gradual edge like (c). Taking difference from the shoulder as the drop solves this problem

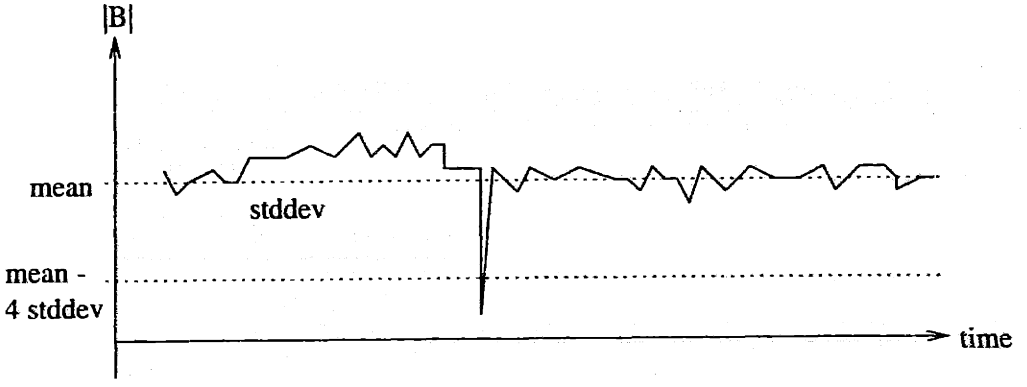


Figure 3-5: Example of a hole

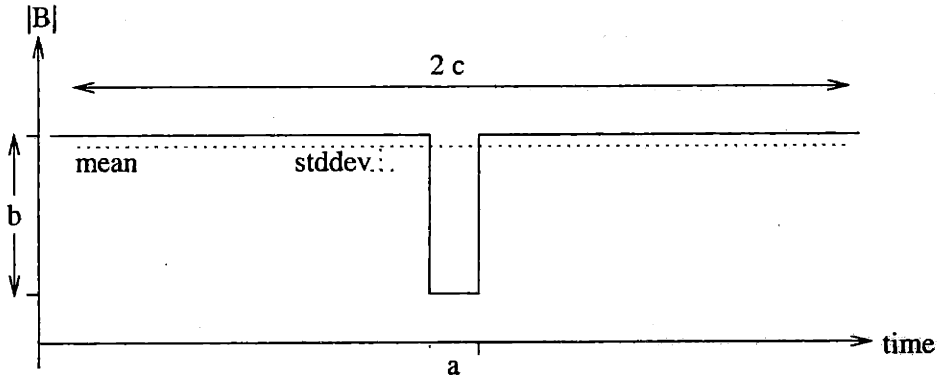


Figure 3-6: A model of a hole

period of $2c$ centered on the hole, $\bar{x}$ is $\frac{ab}{2c}$ below the shoulders, and $\sigma = b\sqrt{\frac{a}{2c}}\sqrt{1-\frac{1}{2c}}$

If we take a drop below $\bar{x} - d\sigma$ as a hole (where $d$ is a constant), to avoid mistaking random noises as a hole, $d$ should be pretty high (more than 3-4).

A chosen $d$ dictates the range that $c$ must be in. Since we want the drop at the hole (1) to be below the threshold depth,

$$b \geq \frac{ab}{2c} + db\sqrt{\frac{a}{2c}}\sqrt{1-\frac{a}{2c}} \tag{3.1}$$

$$\sqrt{\frac{2c}{a}}^2 - d\sqrt{\frac{2c}{a}}\sqrt{1-\frac{a}{2c}} - 1 \geq 0 \tag{3.2}$$

approximating $\sqrt{1-\frac{a}{2c}}$ as 1,

$$\sqrt{\frac{2c}{a}} \geq \frac{1}{2}(d + \sqrt{d^2+4}) \tag{3.3}$$

$$2c \geq \frac{a}{4}(d + \sqrt{d^2+4})^2 \tag{3.4}$$

With pretty high $d$ this is approximately,

$$2c \geq ad^2 \tag{3.5}$$

So, the greater $d$ is, the longer the averaging length ($2c$) needs to be. What's wrong with having a really long $2c$? As Fig. 3-7 shows, if $2c$ is too long, the normal magnetic field level

will change and result in $\sigma$ greater than the local noise we try to measure.

Though $b$ isn't in the equation, it determines how much noise wil increase because of the noise, forcing us to use a higher $2c$.

In practice, we can choose a reasonable value for $d$ and go over several averaging lengths $2c$ to pick up holes of different sizes.

After a few test runs, we find that $d = 4$ and varying $2c$ over a big range gives a reasonable result. For WIND data, we set $2c = 20 \cdot 2^{i/4}$, (rounded to an integer) data points for $i = 0$ to 48. This gives a maximum $2c$ of 81920 data points, and hence the holes we find will have a duration of less than $81920/4^2 = 5120$ data points. Accounting for the approximations in our calculation and the increase in $\sigma$ from the noise, we probably should hope for consistent data for holes up to durations of 2560 data points, which translates to 7680 seconds. For ACE, we set $2c = 20 \cdot 2^{i/4}$ for $i = 0$ to 40, which cover holes of durations up to 640 data points or 9600 seconds. One simply has to try more $2c$ values to extend this range further.

## 3.3 The code

The code follows the idea described, with several details filled in. We first try to find most holes, focusing on missing as few real holes as we can while not worrying much about picking up points that are not a real hole. We later try to filter out these bogus holes. The main procedure written for this purpose is called "find_hole". Its flow is,

```
fh_stddev
fh_pack
cutoff
fh_adjust2
fh_pack
fh_filter_depth
fh_filter_similar
```

Each line lists the name of an IDL procedure we wrote to do the job, in the order. We now go over this in more detail,

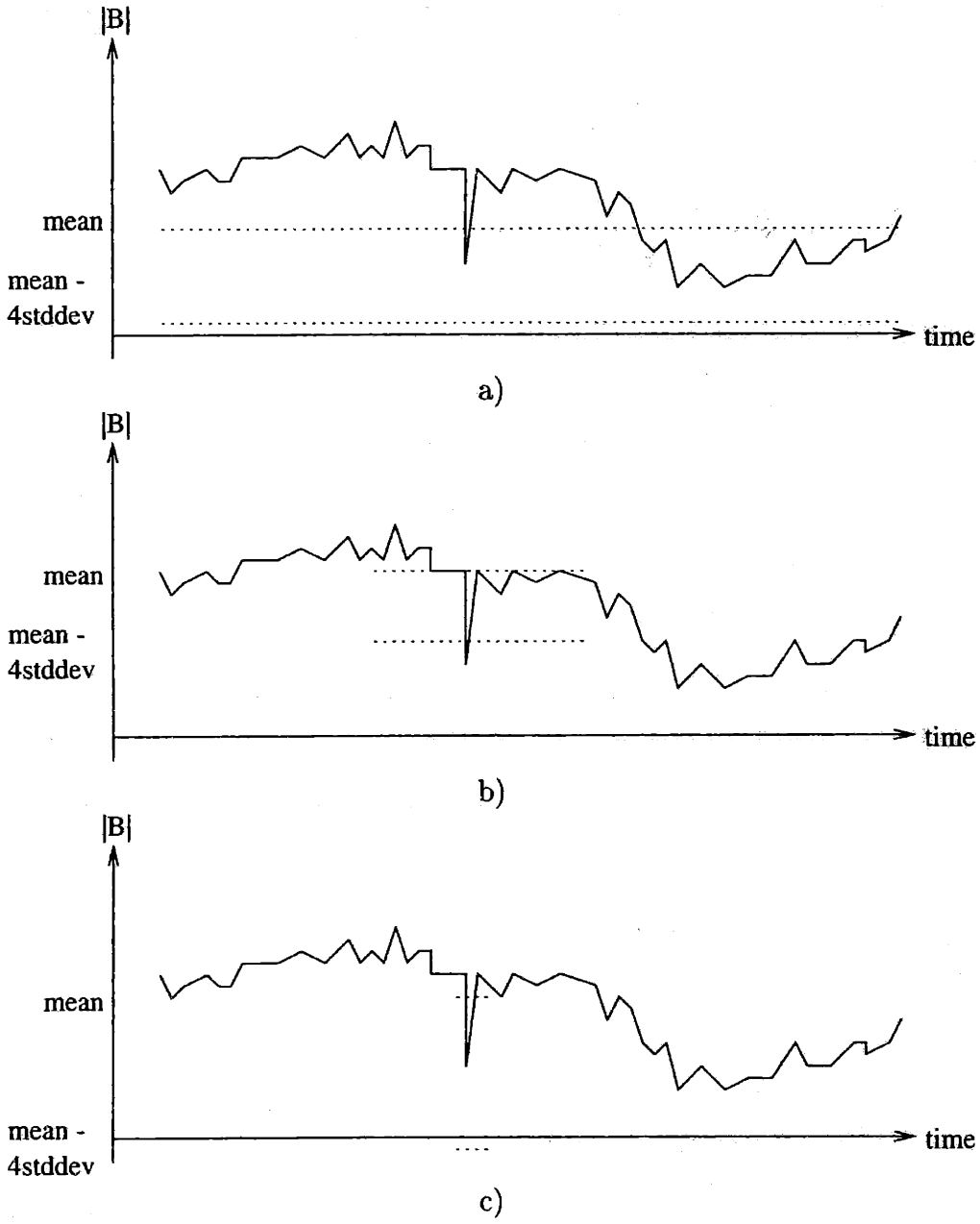


Figure 3-7: Too long (a) and too short (c) averaging length results in a hole drop not making the threshold depth.

**fh_stddev** takes in a requested period and essentially goes over each data point, find $\bar{x}$ and $\sigma$ over several averaging lengths, $2c = (20 \cdot 2^{i/4})$ (rounded to an integer) data points, for $i = 0$ to 40 or 48. Each data point is registered as "part of a hole" if its value is less than $\bar{x} - 4\sigma$. The procedure then lumps consecutive "part of a hole"s together as a hole. Data are loaded a little more than the period requested so we have enough data for the calculations of $\bar{x}$ and $\sigma$.

**fh_pack** grossly goes over the holes found and eliminates some duplicates that result from running many values of $2c$.

**cutoff** drops holes outside the requested period that were found because the extra data was loaded.

**fh_adjust2** tries to guess where each hole starts and ends. Up to now, only points that drop pretty deep are registered as part of the hole. Here, we try to account for points around the edges of the holes, where the data might already start to drop, but haven't got as deep as the center of the hole. If this procedure can't find good starting and ending point of the hole, it assumes that the hole is bogus and ignores that hole.

**fh_pack** is run again to eliminate more duplicates.

**fh_filter_depth** also tries to screen out bogus holes. Only holes that drop lower than 75% of its normal level pass.

**fh_filter_similar** is another attempt to eliminate duplicates. It looks for holes that start and end at about the same point and drops one of them.

With limited computer memory, we ran the code on the data from each year separately. This way, holes that fall between the years are missed out. Since currently we are looking at holes of durations of less than 2-3 hours, this is only a tiny fraction of holes. If one needs to, this can be fixed by running the procedure on periods that go across the year and add that result to what we have.

| year | ACE | | | WIND | | |
|---|---|---|---|---|---|---|
| | count | foy | hole/year | count | foy | hole/year |
| 1995 | | | | 2893 | 0.97 | 2992 |
| 1996 | | | | 8944 | 0.93 | 9584 |
| 1997 | | | | 4927 | 0.95 | 5171 |
| 1998 | 1173 | 0.87 | 1355 | 4917 | 0.96 | 5133 |
| 1999 | 1529 | 1.00 | 1529 | 6369 | 0.73 | 8706 |
| 2000 | 1441 | 1.00 | 1441 | 7205 | 0.86 | 8339 |

Table 3.1: Holes found, fraction of year that data are used (foy), and adjusted holes count per year from ACE and WIND

## 3.4 Result

We inspected several of the holes found and most of what we saw do look like holes. The number of holes that our procedure found is listed in Table. 3.1. Note that we don't have ACE's magnetic field data for the first 49 days of year 1998. WIND's data show only holes that are found when the orbit that is at least 10 Earth radii upstream from an Earth's bowshock model. WIND's magnetic field resolution is about 5 times of ACE's.

Notice that the number of holes per year in WIND varies greatly. It will become evident in later analysis that many of these holes are bogus.

# Chapter 4

# Hole Properties

Here, we play around with the holes we found hoping that we might notice some trends.

## 4.1 Hole Observation Duration

First, we plot the histograms of the duration of the drops in the holes. The "duration" is the time the holes take to pass by the spacecraft.

Since the sampling interval of WIND's magnetic field data we used is 3 seconds, the calculated observation duration value is discrete, i.e. in multiple of $3s$. This quantization can be noticed from a histogram with a bin size considerably smaller $3s$ (Fig. 4-1).

This discreetness arises not only from the sampling rate of the data we use. The time stamp of each data point available to us is in 64-bit IEEE floating point form of "day of year" (doy) format. However, there's evidence that these time stamps went through some 32-bit processing and hence is only 32-bit accurate. Since 32-bit floating point has the mantissa of 24 binary digits, the time stamps holding values as big as 367.0 day are accurate to $367.0/2^{24}$ day, which is equivalent to $1.89s$. When we subtract the time stamps from each other, half of the outcomes that are about $1.89s$ from each other are represented by the same number.

Despite a dip on the left, the observation duration histograms looks exponential, we want to try curve fitting it. The discreetness gives us some problem here. While the histogram like Fig. 4-1 has spikes that form an exponential-looking curve (like 9,6,4,3) it is actually

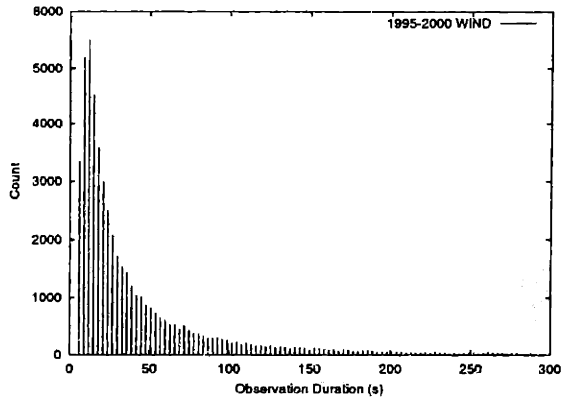


Figure 4-1: Histogram of hole observation duration from WIND from 1995 to 2000. The result is discrete

a mix of zeroes and the spike (like 9,0,0,0,6,0,0,0,4,0,0,0,3,0,0,...). How should we go about curve fitting this kind of data?

One way is to just throw the bins that are zeroes away. One problem is that a spike might occupy two consecutive bins. For an example, spikes like ...,0,0,4,4,0,0,... and ...,0,0,8,0,0,... can arise from the same data with slightly different histogram plotting parameters. The method of throwing zeroes away will cause these two cases to be interpreted very differently.

One can try summing a few spikes into bins to smooth the graph out. For this method to be accurate, the number of spikes in each bin must be about the same. One can try to achieve this by making the bins quite large comparing to the interval between spikes (3$s$ in our WIND data). From Fig. 4-1 it's clear that we are barely able to afford moderate bin size (e.g. 5-6 spikes) while maintaining some statistical accuracy (having several bins that contains more than 10 counts). Alternatively, one try to place the bins at the right places so each bin covers exactly one spike. In the WIND's data we use, this can easily be achieved. This procedure results in Fig. 4-2. Note that the zero in the first bin arises from the fact that the algorithm doesn't allow a hole of size one data point.

At first, we thought that the drop at the beginning of WIND's observation duration histogram was due to the hole search code. It is interesting that similar feature isn't found in ACE's histogram (Fig. 4-3). The turning point might be real, or just a glitch in the hole searching algorithm or how we handle the data. For now, I can't think of how the algorithm

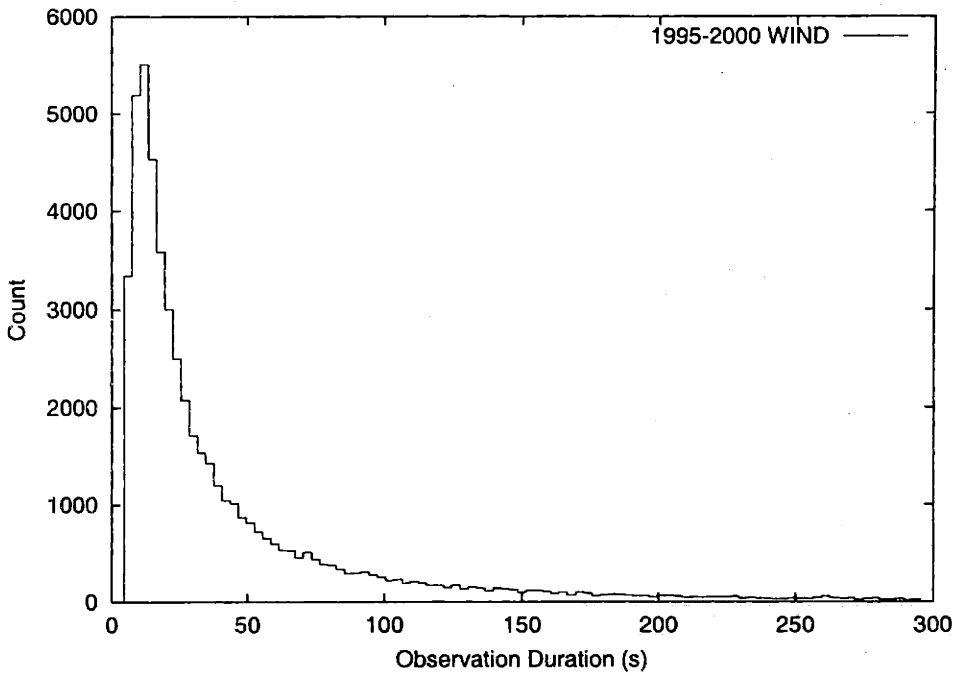


Figure 4-2: A histogram of hole observation duration with proper bin size

can give rise to such the drop in one spacecraft and not the other.

With the first few data points removed and taking square-root of the counts to be the standard deviations, we try to curve fit the histograms to $y = be^{ax}$. The results are shown in Fig. 4-4. For WIND and ACE respectively, decay rates ($a$) are $-0.023$ and $-0.014/s$. Reduced chi squares are 63.87 and 30.73. Evidently the exponential curve doesn't fit well to the data.

If the histograms were exponential, we would expect $a$ from both cases to be about the same. The difference by factor of two that we got is bigger than expected. But seeing that the histograms don't really fit well to the exponential curve anyway, we will ignore that for now.

## 4.2 Hole Length

We now try to look at the length of each hole. We calculate this by multiplying the observation duration by the average solar wind plasma speed across the hole duration. Since we

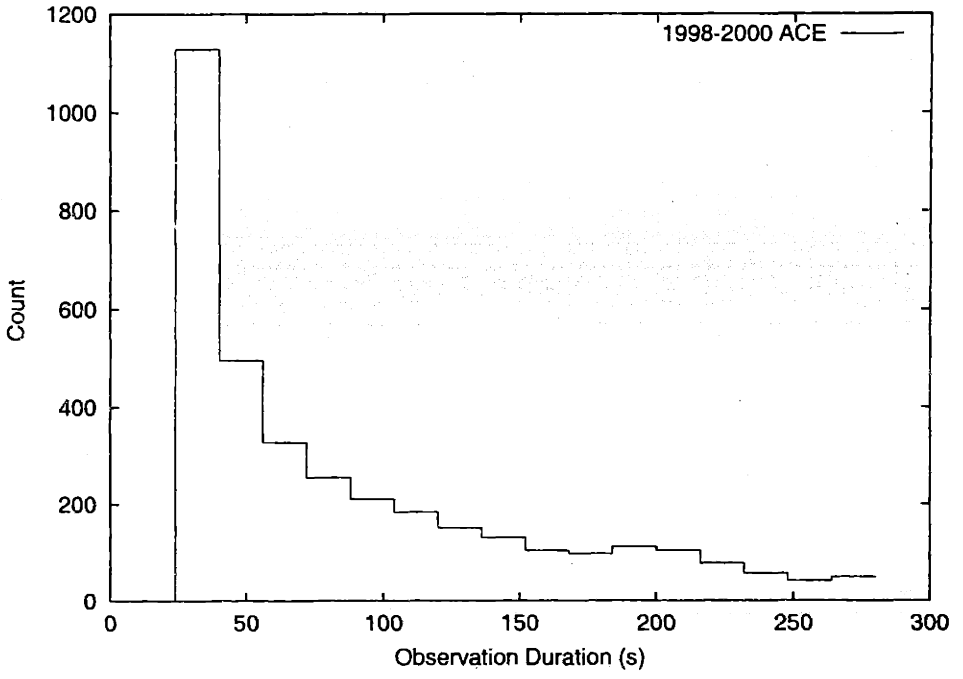


Figure 4-3: Histogram of hole observation duration from ACE from 1998 to 2000.

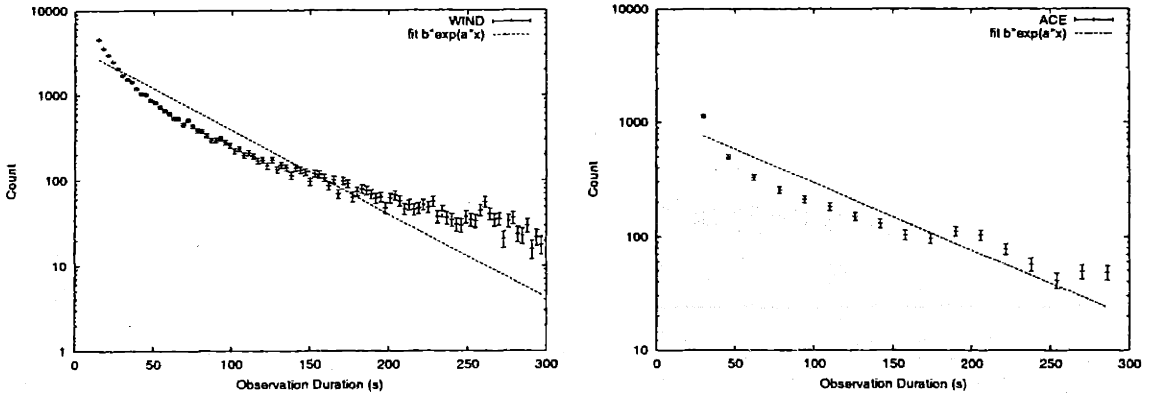


Figure 4-4: Exponential fit to Observation Durations

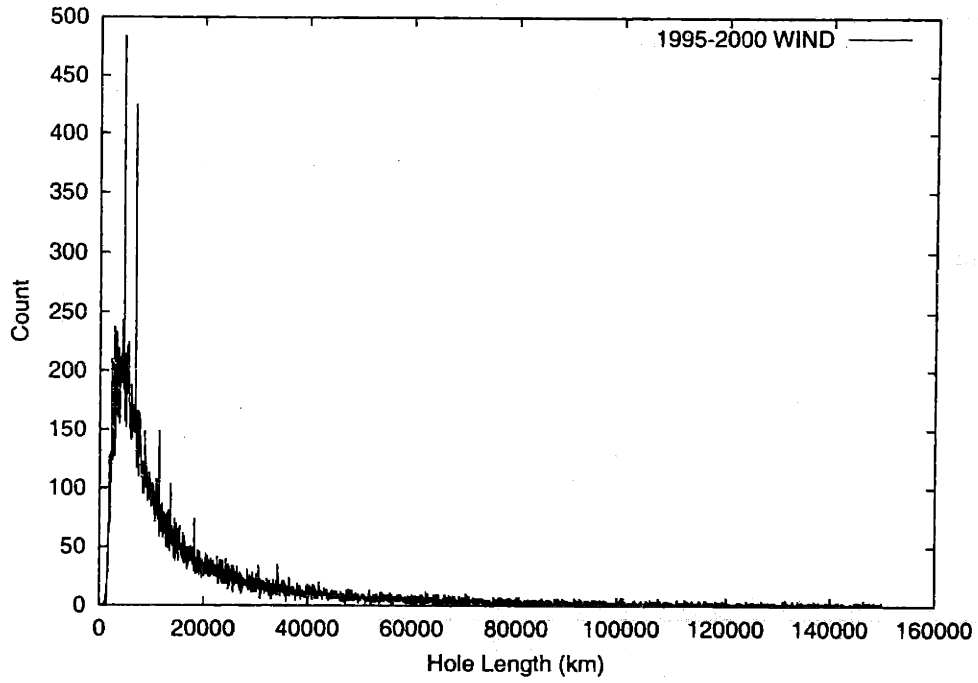


Figure 4-5: Histogram of hole length from WIND from 1995 to 2000.

still don't know the shape of the holes. The length will just be in whatever direction that the solar wind happens to blow by the spacecraft. Once we plot the histogram of the hole lengths (Fig. 4-5), we notice that the plasma speed smoothes out the discreetness previously present in the hole observation durations.

Plotting histograms with larger bins and fitting them to exponential curves ($y = be^{ax}$)–again, cutting off some data at the beginning–gives Fig. 4-6 and Fig. 4-7. For WIND and ACE respectively, fitted $a$ are $-2.14 \times 10^{-5}$ and $-4.31 \times 10^{-5}$, with the reduced chi squares of 42.77 and 7.01.

## 4.3 Duration between each holes

Here, we want to see if hole encounter are truly random (i.e. Poisson process). We plot the time between the beginning of consecutive holes (we will call this "spacing").

The histograms are shown in Fig. 4-8. The sharp peak in WIND's plot is very suspicious and is eventually traced back to several periods, each about a day long, that have a pretty

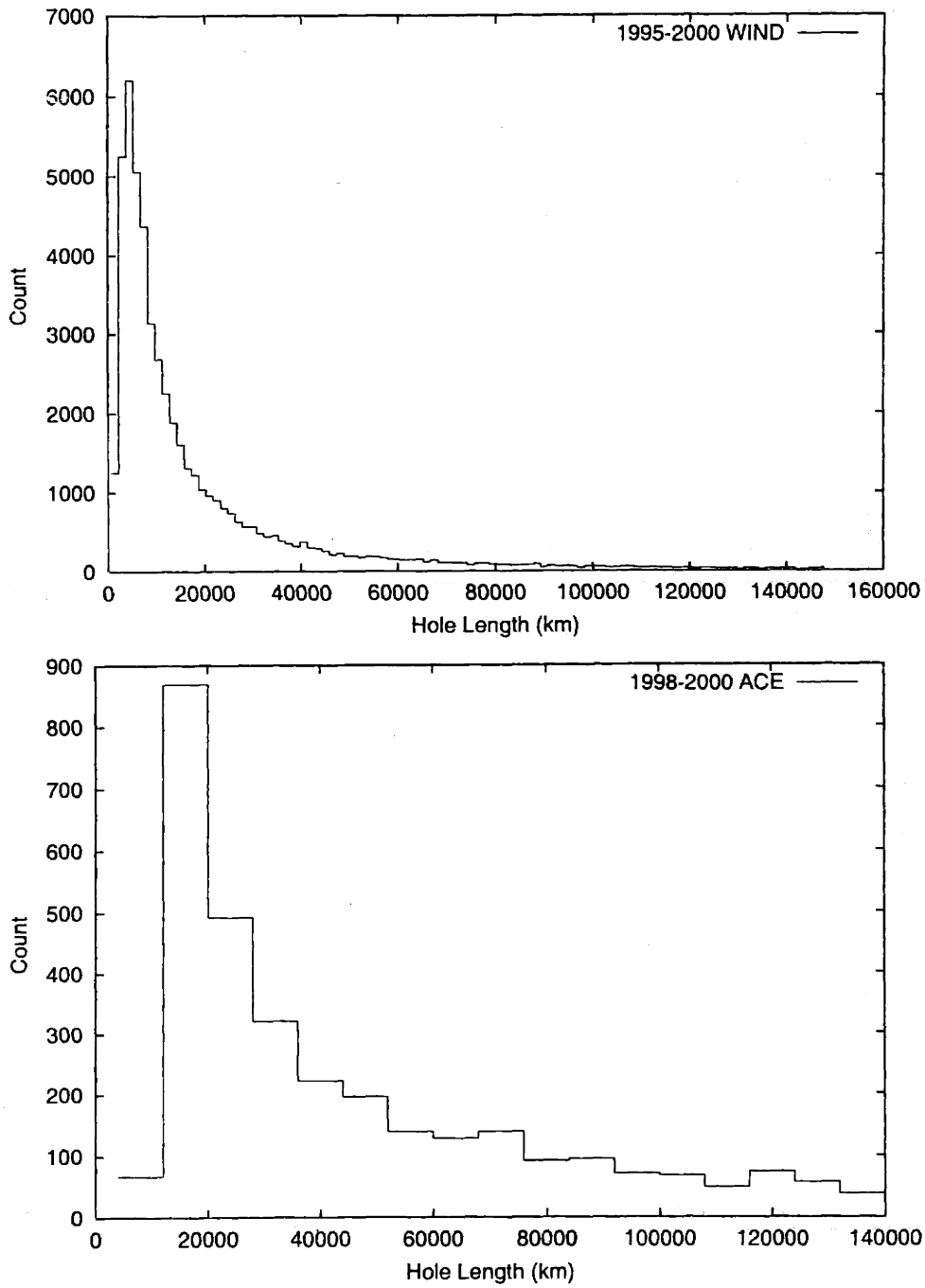


Figure 4-6: Histograms of hole lengths from WIND (1995-2000) and ACE (1998-2000).

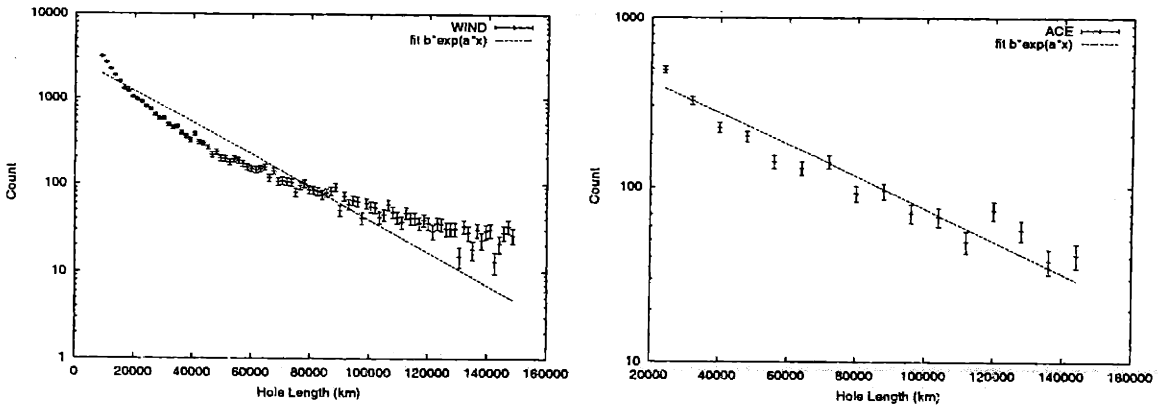


Figure 4-7: Exponential fit to Observation Durations

strange magnetic field data. Some of these periods gives rise to almost a thousand bogus holes in one day. These holes are very close to each other and hence only fall into the first bin or two. We have worked on an additional filter that will screen out these holes. For now, we will have to work with these false holes and treat the results as preliminary.

With the data at the beginning removed, the histograms fit pretty well to exponential curve ($y = be^{ax}$). For WIND and ACE respectively, the fitted $a$ are $-6.14 \times 10^{-5} \pm 0.21 \times 10^{-5}/s$ and $-5.77 \times 10^{-5} \pm 0.26 \times 10^{-5}$, with the reduced chi squares of 2.15068 and 2.41616. The $a$'s found correspond to the expected spacing of $1.63 \times 10^4$ and $1.73 \times 10^4 s$, which translate to 1941 and 1824 holes per year.

Since the exponential curve fits pretty well to our histograms, we might be able to take the calculated expected numbers of holes per year to be our first-order approximation of how many holes we are supposed to find once we rule out the chunks of bogus holes from the mentioned source.

## 4.4 Drop Levels

Fig. 4-10 is the histogram of the ratio between the lowest magnetic field strength registered in each hole and its normal field strength. Note that the peak near 0.7 results from the minimum hole depth that the hole searching algorithm imposes. Fig. 4-11 is the histogram of absolute drops.

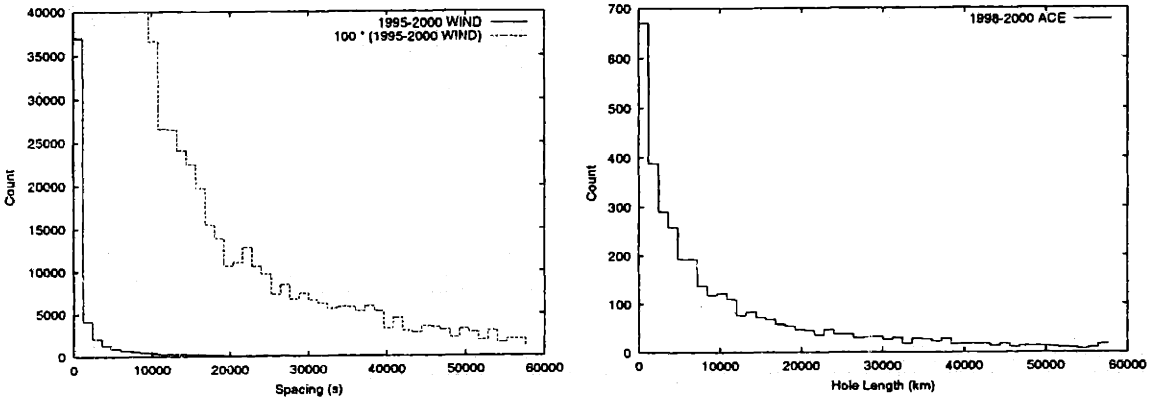


Figure 4-8: Histograms of hole spacing from WIND (1995-2000) and ACE (1998-2000).

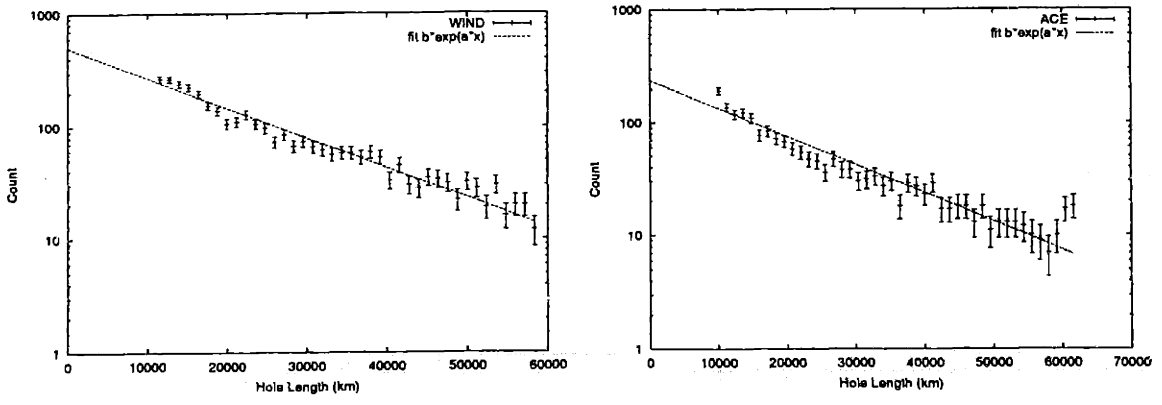


Figure 4-9: Exponential fit to Observation Durations

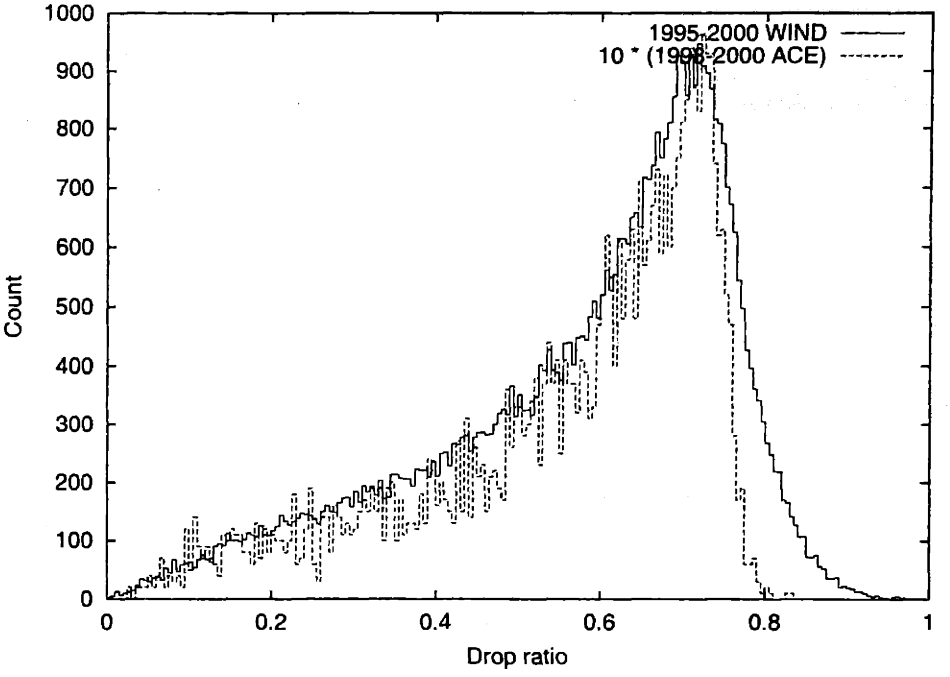


Figure 4-10: Histogram of drop ratio. ACE's counts are multiplied by 10 to scale to WIND's counts.

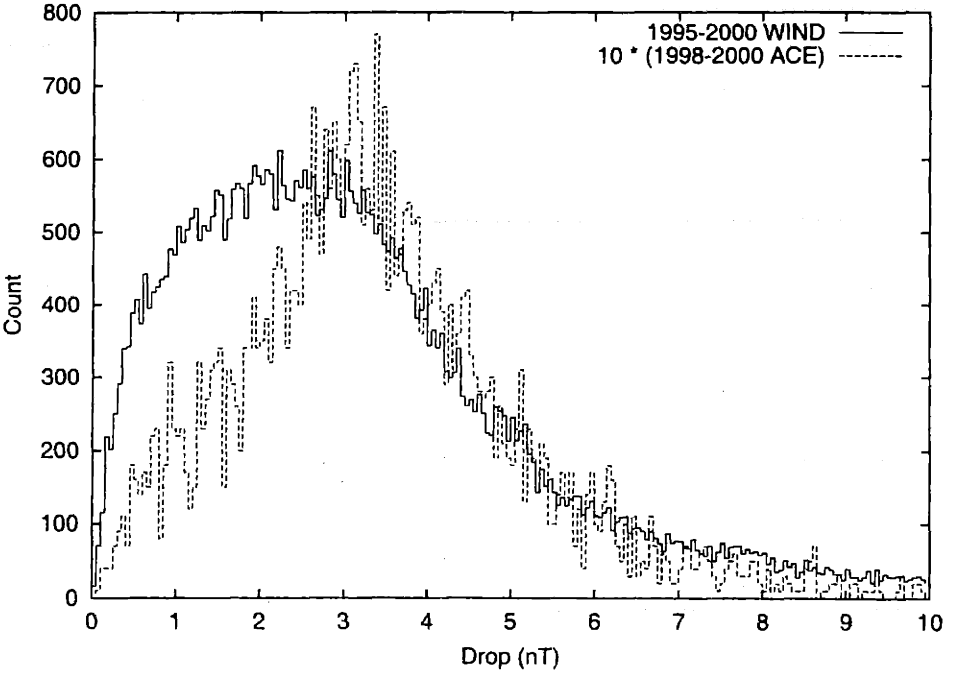


Figure 4-11: Histogram of absolute drop. ACE's counts are multiplied by 10 to scale to WIND's counts.

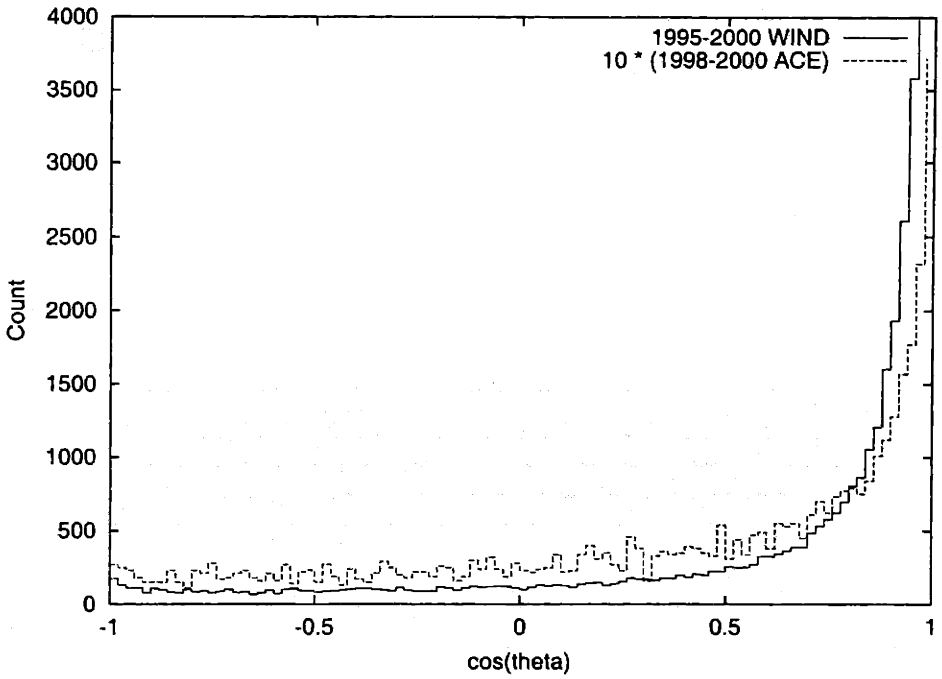


Figure 4-12: Histogram of drop ratio.

## 4.5 Field Direction Change

Fig. 4-12 is the histogram of $cos(\theta)$ where $\theta$ is the angle between the magnetic field directions on each side. Most of the holes we found have $cos(\theta)$ around 1, and hence have the magnetic field on each side of the hole pointing in about the same direction.

# Chapter 5

# Conclusion and Suggestion

To study the statistical characteristics of the magnetic holes, we need a large collection of holes. We come up with a simple way to locate what might be magnetic holes, then refine the method until our collection is good enough for some simple use. We use this collection to analyze basic characteristics of magnetic holes, which, in turn, illuminates us on how to improve the hole collection itself.

With a better collection of holes, we will be able to explore more complex properties of magnetic holes, which hopefully will let us learn more about them, or, at least, improve the quality of our hole collection further.

# Bibliography

[1] WIND Satellite Magnetic Field Investigation
http://lepmfi.gsfc.nasa.gov/mfi/windmfi.html

[2] WIND - Solar Wind Experiment Instrument Page
http://web.mit.edu/space/www/wind/wind_instruments.html

[3] Bartol ACE/Magnetometer Instrument Project Home Page
http://www.bartol.udel.edu:80/čhuck/ace.html

[4] The ACE/Solar Wind Electron, Protron, and Alpha Monitor Page
http://swepam.lanl.gov/